Lasers in Manufacturing Conference 2021

Magnetic field assisted laser ablation of silicon by using short and ultrashort laser pulses

Yiyun Kang[a], Pavel N. Terekhin[b], Garik Torosyan[a], Falicienne G. Keabou[a], Hicham Derouach[a], Mareike Schäfer[a], Bärbel Rethfeld[b], Johannes A. L'huillier[a]

[a]*Photonik-Zentrum Kaiserslautern e.V. and OPTIMAS Research Center, Technische Universität Kaiserslautern, Kohlenhof Straße 10, Kaiserslautern 67663, Germamy*
[b]*Department of Physics and OPTIMAS Research Center, Technische Universität Kaiserslautern, Erwin-Schrödinger-Straße 1, Kaiserslautern 67663, Germany*

Abstract

A controlled machining process with optimum energy-matter coupling in micro-scale by short and ultrashort laser pulses brings great benefits in industrial applications. The influence of external magnetic field on the ablation process of silicon irradiated by laser pulses in the infrared range was investigated. The external field is applied parallel to the laser beam to prevent escaping of the charge carriers in the laser-induced plasma plume from the ablation area. We performed single-pulse irradiation in three different duration ranges: femtosecond, picosecond and nanosecond. We observed that the effect of the external magnetic field depends strongly on the pulse duration. An essential improvement in the efficiency of material removal was achieved for pulses in the nanosecond range.

Keywords: Silicon; magnetic field assisted ablation; short laser pulses; ultrashort laser pulses

1. Introduction

The industrial laser micromachining will highly benefit from the increasing of the processing speed with better quality. The most used methods for achieving it are to increase the average power of the laser source or increase the ablation efficiency per pulse by using different kinds of burst-processing techniques. However, the ability to increase efficiency is still limited with these methods. Therefore, new techniques are needed to further increase the laser performance for numerous applications. We propose an approach, which is based on the application of an external magnetic field in the direction of the laser beam on the laser processing plane. Previous research already proved a significant enhancement on the ablation with the magnetic field assistance [Farrokhi et al., 2016; Farrokhi et al., 2019; Tang et al., 2019; Maksimovic et al., 2019; Maksimovic et al., 2020; Zhang et al, 2021], especially in the drilling process [Ye et al., 2013; Ho et al., 2014].

In our approach, we irradiate silicon samples by laser pulses with durations from femtoseconds to nanoseconds accompanied by the externally applied axial magnetic field. Single-pulse measurements are carried out with and without a magnetic field. Since different pulse durations induce different excitation processes on the same material [Rethfeld et al., 2004], the effects do also vary from the pulse duration and the magnetic field strength.

2. Experimental setup

The experiments with three different pulse durations are performed on different laser setups. The femtosecond laser used in the experiments is a fiber laser system (BlueCut, Menlo Systems GmbH). The laser emits pulses of 400 fs at Full Width Half Maximum (FWHM) with linearly polarized light at a central wavelength of approximately 1030 nm. The picosecond laser (Hyper Rapid 25, Coherent Kaiserslautern GmbH) has a pulse width of 10 ps at FWHM. The experiments were operated with a wavelength of 1064 nm. Additionally, the nanosecond laser (Impress, XITON Photonics GmbH) generates the laser pulses with a duration of 7 ns and a wavelength of 1064 nm.

A galvanometric scanner system (hurrySCANR©II/14, SCANLAB AG) with telecentric F-theta optics (f≈100 mm, Linos respectively Jenoptik AG) was used for deflecting and focusing the beam onto the workpiece. To determine the laser spot size in the focal plane, the fit method from Liu [Liu, 1982] was applied and the obtained spot radii ($1/e^2$ of the maximum) are summarized in Table 1.

Table 1. Laser parameters.

Laser systems	Pulse duration	Wavelength (nm)	Maximum Pulse energy (µJ)	Pulse repetition rate (kHz)	Spot radius on workpiece (µm)
BlueCut	400 fs	1030	10	10	9.5
Hyper RAPID 25	10 ps	1064	80	12.5	8.9
Impress	7 ns	1064	120	10	12.5

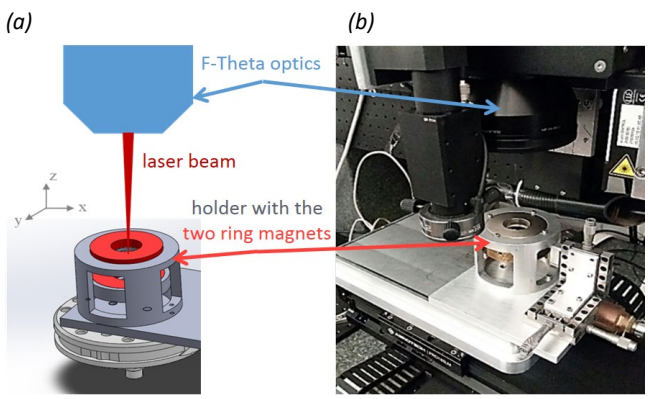

Fig. 1. (a) The scheme of the setup with an external magnetic field. (b) A Sketch of the experimental setup.

We apply the magnetic field with the flux direction along the laser beam. A setup consists of two ring magnets which are attached to a holder with the sample at the center between the magnets (Fig. 1). The top magnet is fixed. The magnetic field strength is controlled by changing the position of the bottom magnet. As

a result, we can reach a homogeneous magnetic flux with an area of 10 x 10 mm^2 at the center, where our sample is located.

3. Results and discussion

The ablation threshold fluence on silicon for single-pulse irradiation for different pulse durations is measured using Liu's method [Liu, 1982]. All the ablation thresholds are determined without a magnetic field. The ablation thresholds are 0.57 J/cm^2, 1.05 J/cm^2, 4.07 J/cm^2 by femtosecond laser, picosecond laser and nanosecond laser, respectively. By comparing the ablation threshold for the three pulse durations, its values increases with increasing the laser pulse duration, as was already reported [Wang et al., 2010].

For the ablation study, single-pulse experiments are carried out on silicon samples with and without a magnetic field. The applied magnetic field flux density is 200 mT. As a result, the change of the ablation diameter, and the change of the ablation depth are compared to the ablation without a magnetic field. The crater morphologies are also analyzed. The change of the ablation diameter *D* and the change of the ablation depth *h* are calculated using the equations (1), and (2). The craters are investigated using a scanning electron microscope (SEM; EVO-MA10, Carl Zeiss Microscopy GmbH)) and a light microscope (Axio Imager.M2m, Carl Zeiss Microscopy GmbH) to verify the change obtained on the crater morphology.

$$\text{relative change of the ablation diameter} = \frac{D(\text{with magnetic field}) - D(\text{without magnetic field})}{D(\text{without magnetic field})} * 100\% \quad (1)$$

$$\text{relative change of the ablation depth} = \frac{h(\text{with magnetic field}) - h(\text{without magnetic field})}{h(\text{without magnetic field})} * 100\% \quad (2)$$

3.1. Results from fs laser ablation

As we have mentioned above, the change of the ablation diameter and the ablation depth in the single-pulse ablation were investigated and are plotted for fs excitation in Fig. 2. In general, the strongest impact is noticed at the region close to the threshold fluence. The reduction of the crater diameters with an external magnetic field is observed.

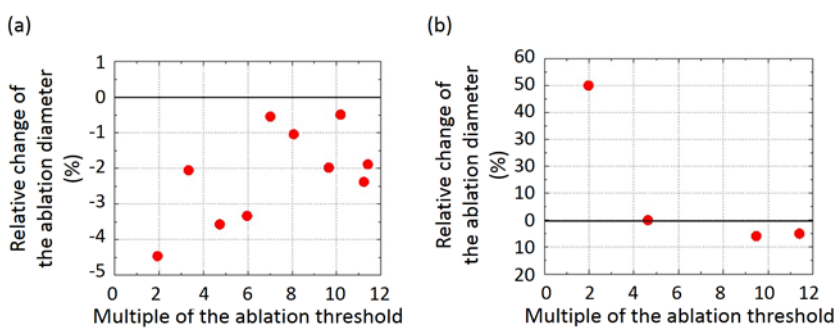

Fig. 2. The single-pulse ablation with the femtosecond laser. (a) The relative change of the ablation diameter; (b) The relative change of the ablation depth.

At lower fluence, the difference is the biggest, around 5 %. The difference is close to 0 when the fluence is more than 6 times above the ablation threshold. However, the maximal difference is still in a small range, less than 5 %. Regarding the change in the removal depth, a clear tendency shows up. The magnetic field enhances the ablation depth at the low fluence regime. The crater ablated with 200 mT is 50 % deeper than the crater without an applied magnetic field when the laser fluence is twice the threshold fluence. When the fluence is more than 4 times of ablation threshold, the difference of the crater depth generated by magnetic field is neglectable.

3.2. Results from ps laser ablation

Fig. 3 shows the relative change in the diameter and the removal depth of ablated craters in the ps regime.

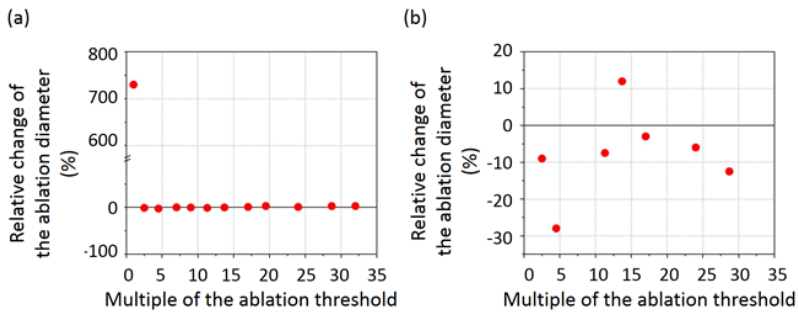

Fig. 3. The single-pulse ablation with the picosecond laser. (a) The relative change of the ablation diameter; (b) The relative change of the ablation depth.

The diameters of the craters are 7-8 times bigger with an applied magnetic field compared to the case without a magnetic field at low incident fluence. With the further increase in the laser fluence, the change of the diameter is within ± 5%. When evaluating the relative change in the removal depth of the single pulse ablated craters, the removal depth with the help of 200 mT is 10% - 30% shallower. By higher fluence (> $5*F_{th}$), the difference is constant and around 10% smaller with magnetic field-assisted ablation.

To analyze the crater morphology SEM pictures are taken and are illustrated in Fig. 4. Based on these SEM pictures it is obvious that the ablation area at $1.04*F_{th}$ is significantly bigger with the external magnetic field compared to the case without an applied magnetic field.

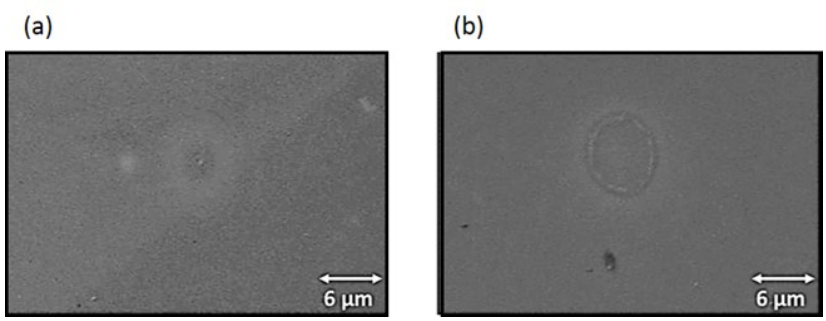

Fig. 4. SEM pictures of single-pulse ablated points close to the threshold fluence by the excitation with ps-pulses.
(a) B=0 mT; (b) B=200 mT.

3.3. Results from ns laser ablation

The change of the ablation diameter, as shown in Fig. 5, has a clear trend of changing, which makes it possible to control the diameter of the ablated crater with a magnetic field in the following study. A significant increase of the ablation diameter of 6 times bigger with magnetic field happens at the threshold fluence. With further increasement of the applied pulse energy, the effect drops dramatically. However, the enhancement tends to be higher with the fluence smaller than 4 times the threshold fluence compared with the high fluence. By the change of the removal depth, the crater with the magnetic field assistance is at all times deeper up to 40 %. It seems to be constantly changing without much influence from laser fluence.

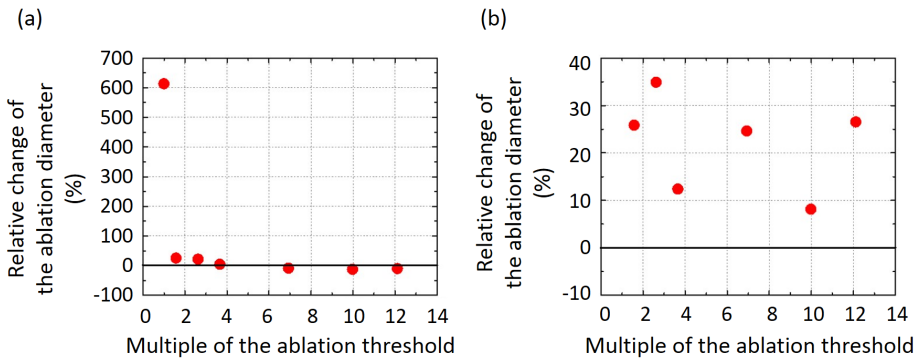

Fig. 5. The single-pulse ablation with nanosecond laser. (a) The change of the ablation diameter; (b) The change of the ablation depth.

The light microscope pictures are taken to show the crater at the ablation threshold with and without magnetic field in Fig. 6. A strong ablation is noticed when the magnetic flux density of 200 mT is applied on the sample surface, while only a moderate ablation is seen by the normal ablation.

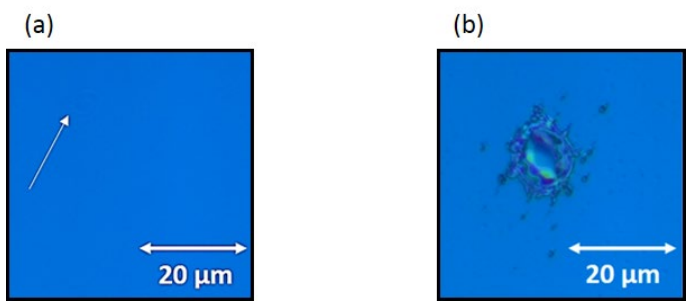

Fig. 6. Light microscope pictures of single-pulse ablated points at the threshold fluence. (a) B=0 mT; (b) B=200 mT.

To sum up the results from a single pulse ablation on silicon discussed above, the magnetic field has a strong effect on the ablation with low fluence near the ablation threshold. By applying a magnetic field with a flux density of 200 mT to the ablation process, the sizes of the ablated craters are dramatically wider, up to 7 times. Moreover, partly the ablation depth could also be enhanced. This effect of an enhanced ablation process significantly increases by the excitation with long pulse durations compared to the excitation with sub-ps-pulses.

The mechanism of the material excitation with a nanosecond laser is relatively different from ultrashort laser pulses in femtosecond and picosecond ranges. More heat is conducted to the material by the longer

pulse width in the nanosecond scale. The external magnetic field determines the motion of the plasma generated during laser irradiation. During the nanosecond laser pulse, the plasma is already generated on the processed area. Instead of the free expanding, the plasma is confined at the middle of the crater area and rotates around the laser beam by the force generated with a magnetic field. It leads to a better heat accumulation in the center of the crater to process deeper.

Nonetheless, the positive effect of field-assisted ablation due to an applied magnetic field by the excitation with sub-ps-pulses is evident. Whereby this behavior will be significantly improved by multi-pulse ablation. Moreover, the rim formation and surface modification by debris formation could be influenced by an applied magnetic field during the ablation process. Fig. 7 illustrates an example of the ablated crater by using a multiple of fs-pulses on the sample. In the presence of a magnetic field, no rim formation occurs, whereas a high rim with melt droplets were developed if no magnetic field has assisted the ablation process. For a detailed understanding of the existing mechanism by an applied magnetic field by the excitation of multi-pulses with sub-ps-pulse duration additional work is in progress and is out of scope of the current work.

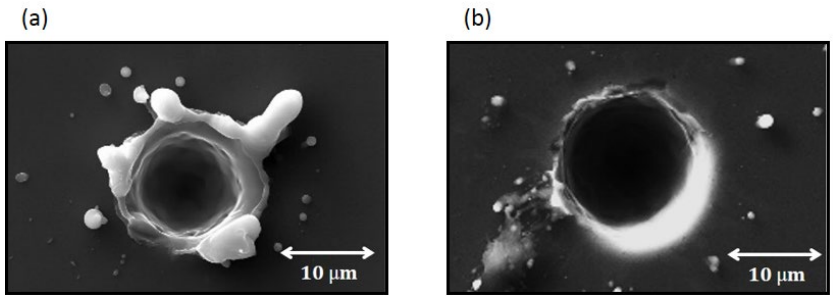

Fig.7. SEM pictures of 10-pulse ablated points at 2 times of the ablation threshold. (a) B=0 mT; (b) B=200 mT.

4. Conclusion

We show that a constant external magnetic field can significantly influence the ablation process from the pulse duration of fs to ns range. In all pulse ranges, the strongest effect is happening at the low fluence regime, especially near the threshold fluence. The ablation can be enhanced up to 6-7 times when a magnetic field with a flux density of 200 mT is applied. The longer the pulse duration, the greater effect is seen. By ns laser ablation, a clean crater with a deeper profile without a rim is formed with the help of the external magnetic field. A clear improvement in quality and speed of ablation by ns pulses can be concluded. The improvement is supposed to be attributed to the confinement of laser-produced plasma by the magnetic field and specific propagation effects in the magnetized plasma. With the axial magnetic field, the laser-induced plasma will rotate around the laser beam while propagating deeper into the material. The debris is caught by the moving plasma while creating a deeper crater.

Acknowledgements

The project was supported by Bundesministerium für Bildung und Forschung – BMBF with the project number of 13N14867. The authors thanks Hochschule Kaiserslautern (Specially Prof. Peter Starke) for providing the possibility to carry out an analysis on a confocal microscope.

References

Farrokhi, H., Gruzdev, V., Zheng, H. Y., Rawat, R.S., Zhou, W., 2016. Magneto-absorption effects in magnetic-field assisted laser ablation of silicon by UV nanosecond pulses. Applied Physics Letters 108, 254103. https://doi.org/10.1063/1.4954708

Farrokhi, H., Gruzdev, V., Zheng, H., Zhou, W., 2019. Fundamental mechanisms of nanosecond-laser-ablation enhancement by an axial magnetic field, J. Opt. Soc. Am. B 36, pp. 1091-1100. https://doi.org/10.1364/JOSAB.36.001091

Ho, C.-C., Tseng, G.-R., Chang, Y.-J., Hsu, J.-C., Kuo, C.-L.,2014. Magnetic-field-assisted laser percussion drilling, Int J Adv Manuf Technol 73, pp. 329–340. https://doi.org/10.1007/s00170-014-5815-6

Liu, J. M., 1982. Simple technique for measurements of pulsed Gaussian-beam spot sizes, Opt. Lett. 7, pp. 196-198. https://doi.org/10.1364/OL.7.000196

Maksimovic, J., Ng S.-H., Katkus T., Cowie B.C.C., Juodkazis S., 2019. External Field-Controlled Ablation: Magnetic Field. Nanomaterials 9(12), p.1662. https://doi.org/10.3390/nano9121662

Maksimovic, J., Ng, S.-H., Katkus, T., An Le, N.H., Chon, J.W.M., Cowie, B.C.C., Yang, T. Bellouard, Y., Juodkazis, S., 2020. Ablation in Externally Applied Electric and Magnetic Fields, Nanomaterials 10, p. 182. https://doi.org/10.3390/nano10020182

Rethfeld, B., Sokolowski-Tinten, K., von der Linde, D. and Anisimov, S.I., 2004. Timescales in the response of materials to femtosecond laser excitation. Applied Physics A 79(4), pp.767–769. https://doi.org/10.1007/s00339-004-2805-9

Tang, H., Qiu, P., Cao, R., Zhuang, J., Xu, S., 2019. Repulsive magnetic field–assisted laser-induced plasma micromachining for high-quality microfabrication, Int J Adv Manuf Technol 102, pp. 2223–2229. https://doi.org/10.1007/s00170-019-03370-5

Wang, X., Shen, Z. H., Lu, J., Ni, X. W., 2010. Laser-induced damage threshold of silicon in millisecond, nanosecond, and picosecond regimes. Journal of Applied Physics 108 (3), 033103. https://doi.org/10.1063/1.3466996

Ye, C., Cheng, G. J., Tao, S., Wu, B., 2013. Magnetic Field Effects on Laser Drilling. ASME. J. Manuf. Sci. Eng. 135(6), 061020. https://doi.org/10.1115/1.4025745

Zhang, Y., Zhang, Z., Zhang, Y., Liu, D., Wu, J., Huang, Y., Zhang, G., 2021. Study on machining characteristics of magnetically controlled laser induced plasma micro-machining single-crystal silicon, Journal of Advanced Research 30, pp. 39-51. https://doi.org/10.1016/j.jare.2020.12.005